Structural Locus of the pH Gate in the Kir1.1 Inward Rectifier Channel

Henry Sackin,* Mikheil Nanazashvili,* Lawrence G. Palmer,[†] M. Krambis,* and D. E. Walters*

*Department of Physiology and Biophysics, The Chicago Medical School, North Chicago, Illinois; and [†]Department of Physiology and Biophysics, Weill Medical College of Cornell University, New York, New York

ABSTRACT   The closed-state crystal structure of prokaryotic inward rectifier, KirBac1.1, has implicated four inner helical phenylalanines near the cytoplasmic side as a possible locus of the channel gate. In the present study, we investigate whether this structural feature corresponds to the physiological pH gate of the renal inward rectifier, Kir1.1 (ROMK, KCNJ1). Kir1.1 is endogenous to the mammalian renal collecting duct and the thick ascending limb of Henle and is strongly gated by internal pH in the physiological range. It has four leucines (L160-Kir1.1b), homologous to the phenylalanines of KirBac1.1, which could function as steric gates near the convergence of the inner (M2) helices. Replacing these Leu-160 residues of Kir1.1b by smaller glycines abolished pH gating; however, replacement with alanines, whose side chains are intermediate in size between leucine and glycine, did not eliminate normal pH gating. Furthermore, a double mutant, constructed by adding the I163M-Kir1.1b mutation to the L160G mutation, also lacked normal pH gating, although the I163M mutation by itself enhanced the pH sensitivity of the channel. In addition to size, side-chain hydrophobicity at 160-Kir1.1b was also important for normal pH gating. Mutants with polar side chains (L160S, L160T) did not gate normally and were as insensitive to internal pH as the L160G mutant. Hence, either small or highly polar side chains at 160-Kir1.1b stabilize the open state of the channel. A homology model of the Kir1.1 closed state, based on the crystal structure of KirBac1.1, was consistent with our electrophysiological data and implies that closure of the Kir1.1 pH gate results from steric occlusion of the permeation path by the convergence of four leucines at the cytoplasmic apex of the inner transmembrane helices. In the open state, K crosses the pH gate together with its hydration shell.

INTRODUCTION

ROMK (Kir1.1), expressed on the surface of *Xenopus laevis* oocytes, displays kinetic and permeation properties characteristic of the weak inward rectifier channel that mediates K secretion in the mammalian cortical collecting tubule and K recycling in the mammalian thick ascending limb of the loop of Henle (Palmer et al., 1997). At the normal intracellular pH of oocytes, ROMK is open >90% of the time (Choe et al., 1997).

Intracellular acidification shuts down ROMK by a cooperative process with an apparent Hill coefficient of ~3 (Tsai et al., 1995; Doi et al., 1996; Leipziger et al., 2000; McNicholas et al., 1998; Sackin et al., 2001; Chanchevalap et al., 2000). This probably accounts for the decrease in renal K secretion observed during acidosis (Malnic et al., 1966).

Intracellular pH is primarily sensed by an N-terminal lysine (Kir1.1b-K61) in the first transmembrane-spanning α-helix (Fakler et al., 1996; Choe et al., 1997; Schulte et al., 1999), although other residues in both the N- and C-terminal regions also modulate the sensitivity of the channel to internal pH (Choe et al., 1997; Schulte et al., 1999; Chanchevalap et al., 2000). The physical gate, responsible for channel closure during internal acidification, is believed to be structurally distinct from the pH sensor.

Elucidation of the crystal structure of the prokaryotic bacterial channel KirBac1.1 (Kuo et al., 2003) suggests that the Kir1.1 gate might be centered at a single residue (L160-Kir1.1b), corresponding to F146 in KirBac1.1. This site is close to the crossing of inner helical bundles at the cytoplasmic end of the transmembrane permeation path. In the present study, we utilized electrophysiological measurements and site-directed mutagenesis to evaluate whether L160-Kir1.1b was a crucial element of the inward rectifier gate.

METHODS

Mutant construction and expression of channels

Point mutations in Kir1.1b (ROMK2; EMBL/GenBank/DDBJ accession No. L29403) were engineered with a PCR QuikChange mutagenesis kit (Stratagene, La Jolla, CA), using primers synthesized by IDT (Integrated Data Technologies, Coralville, IA). Nucleotide sequences were checked on an Applied Biosystems 3100 DNA sequencing machine at the University of Chicago Cancer Research Center (Applied Biosystems, Foster City, CA).

Plasmids were linearized with *Not*I restriction enzyme and transcribed in vitro with T7 RNA polymerase in the presence of the GpppG cap using the mMESSAGE mMACHINE kit (Ambion, Austin, TX). Synthetic cRNA was dissolved in water and stored at −70°C before use. Stage V–VI oocytes were obtained by partial ovariectomy of female *Xenopus laevis* (NASCO, Ft. Atkinson, WI), anesthetized with tricaine methanesulfonate (1.5 g/L, adjusted to pH 7.0). Oocytes were defolliculated by incubation (on a Vari-Mix rocker) in Ca-free modified Barth's solution (82.5 mM NaCl, 2 mM KCl, 1 mM MgCl2, and 5 mM HEPES, adjusted to pH 7.5 with NaOH) containing 2 mg/ml collagenase type IA (Cat# C9891, Sigma Chemical, St. Louis, MO) for 90 min, and, if necessary, another 90 min in a fresh enzyme solution at 23°C. Oocytes were injected with 0.5–1 ng of cRNA and incubated at 19°C in 2× diluted Leibovitz medium (Life Technologies, Grand Island, NY) for 1–3 days before measurements were made.

All experiments described were conducted at room temperature (21 ± 2°C) on ROMK2 (or mutants of ROMK2) expressed in *Xenopus* oocytes.

Before either whole-cell or patch-clamp experiments (described below), all oocytes were pre-incubated in 100-mM K solutions (50 mM Cl + 50 mM acetate) for 2 h at pH 7.8. This compensated for prior exposure of oocytes to low external K during the period of exogenous expression and insured that both wild-type and mutant oocytes had reproducible responses to pH.

Whole-cell experiments

Whole-cell currents and conductances were measured in intact oocytes using a two-electrode voltage clamp (Model CA-1, Dagan, Minneapolis, MN) with 16 command pulses of 30-ms duration between -200 mV and $+100$ mV, centered around the resting potential. Oocytes expressing ROMK or mutants of ROMK were bathed in permeant acetate buffers to control their internal pH as previously described (Doi et al., 1996; Leipziger et al., 2000; Choe et al., 1997). The composition of the bath for the whole-cell experiments was: 50 mM KCl, 50 mM K acetate, 1 mM MgCl₂, 2 mM CaCl₂ 5 mM HEPES, and 1 mM SITS (4-acetamido-4-isothiocyanostilbene-2,2′-disulfonic acid). SITS was used to minimize small endogenous chloride currents; however, batches of oocytes exhibiting chloride currents >1 μA were discarded, as were oocytes that did not exhibit at least a 40-mV shift in membrane potential for a 10-fold change in external [K].

The relation between intracellular and extracellular pH was calculated from a previous calibration with ROMK oocytes: $pH_i = 0.595 \times pH_o + 2.4$ (Choe et al., 1997). Earlier studies have indicated that Kir1.1 inward conductances were essentially insensitive to external pH (Tsai et al., 1995). All currents were normalized to the maximum whole-cell current for that oocyte to compensate for differences in expression efficiency between wild-type and mutant channels.

Patch-clamp experiments

Cell-attached recordings were used to maximize channel stability and avoid dephosphorylation-induced rundown that often occurred with excised patches of Kir1.1 (MacGregor et al., 1998; McNicholas et al., 1994, 1996). The pH on the cytoplasmic side of the patch was controlled by controlling internal oocyte pH, using either 10-mM or 100-mM K permeant acetate buffers in the bath, together with 0-mM Mg and 2-mM Ca (Choe et al., 1997; Tsai et al., 1995). Osmolarity was adjusted to 205 ± 5 mOsmol/L with NaCl. At the bath-flow rates used, 5–10 min were required to change internal pH to a new steady-state value. The pH on the extracellular side of the patch was held constant at 7.8 using 100 mM KCl, HEPES-buffered, pipette solutions containing either no divalents, or 1 mM Mg and 2 mM Ca.

Determinations of channel activity were conducted exclusively on inward currents since these give clear, well-defined transitions between open and closed states. The high open probability of Kir1.1 channels made it relatively easy to determine the number of active channels in a given patch. Only patches containing a single channel were used for kinetic analyses of ROMK and the L160 mutants.

Patch-clamp pipettes were pulled from 75-mm borosilicate glass (#G85165T-3, Warner Instrument, Hamden, CT) using a two-stage process (L/M-3P-A puller) and coated with Sylgard (Dow Corning, Midland, MI). In all patch-clamp experiments, the vitelline membrane was first removed with forceps after a brief exposure to hypertonic (450 mOsmol/L) solution.

Pipette resistances ranged from 5 to 10 MΩ. Currents were recorded with a Dagan 8900 patch-clamp amplifier and stored, unfiltered, on videotape using Instrutech hardware (VR-10B and ITC-16, InstruTECH, Port Washington, NY). Single-channel events were sampled at 5 kHz and analyzed off-line using Bruxton software (Acquire 4.0.10 and Tac/TacFit 4.1.5, Bruxton, Seattle, WA). All statistical comparisons were conducted using Statview 5.05 software (SAS Institute, Cary, NC).

Homology model

To facilitate interpretation of the electrophysiological results, we made a homology model of the Kir1.1b sequence along the inner transmem-

brane helices (from A137-Kir1.1b to I163-Kir1.1b) onto the x-ray crystal structure of the closed state of KirBac1.1 (1P7B, Kuo et al., 2003), near the putative pH gate using the *Molecular Operating Environment* software, Ver. 2003.02 (Chemical Computing Group, Montreal, Canada). The orientation of the Kir1.1b side chains was determined from a library of conformations, followed by 100 cycles of energy minimization to alleviate bad steric contacts.

RESULTS

ROMK is a pH-gated channel

Previous studies have indicated that ROMK (Kir1.1) has a strong sensitivity to internal pH (Tsai et al., 1995; Fakler et al., 1996; Choe et al., 1997; McNicholas et al., 1998; Chanchevalap et al., 2000), but almost no sensitivity to external pH for inward currents (Tsai et al., 1995). This was confirmed in the present study using *Xenopus* oocytes expressing wild-type ROMK. Channels were recorded in cell-attached patches to avoid rundown (McNicholas et al., 1994, 1996; MacGregor et al., 1998), and permeant (acetate) buffers were used to modify internal pH. In this manner, internal oocyte pH could be controlled from 6.0 to 7.6 (see Methods for calibration).

Decreasing oocyte pH reversibly decreased the number of active ROMK2 (Kir1.1b) channels (Fig. 1 *A*). At an internal pH of 6.3, the normally high P_o of this channel abruptly decreased to zero without discernable changes in single-channel kinetics until the point of final closure.

The average timecourse for pH-dependent closure of ROMK channels was quite reproducible (Fig. 1 *B*), and probably reflects the time required to acidify the oocyte using permeant acetate buffers. The high P_o of the Kir1.1 channel family facilitates counting individual channels, provided the number of active channels in a patch does not exceed 10. Elevating internal pH consistently restored channel activity (Fig. 1 *B*), whereas the shaded area in the figure denotes one standard error above the mean level of channel activity. Previous studies with excised macropatches suggest that this change in channel activity represents gating of individual ion channels rather than an insertion-and-retrieval process (Schulte et al., 2001).

Subconductance levels were sometimes seen, immediately before channel closure (Fig. 1 *A, inset*). This has also been reported by other investigators (MacGregor et al., 1998). On the average (Table 1), the wild-type ROMK channels in this study had an open probability of 0.91 ± 0.01 ($n = 5$), characterized by a single open state with mean dwell time of 20.6 ± 0.3 ms ($n = 5$) and a single closed state with mean closed time of 1.6 ± 0.2 ms ($n = 5$). This was not significantly different from ROMK single-channel kinetics at low pH, immediately before channel closure (compare Tables 1 and 2).

In some cases, a second closed state was seen at large negative cell potentials. This second (longer) closed state reflected block by low levels of contaminant divalents in the
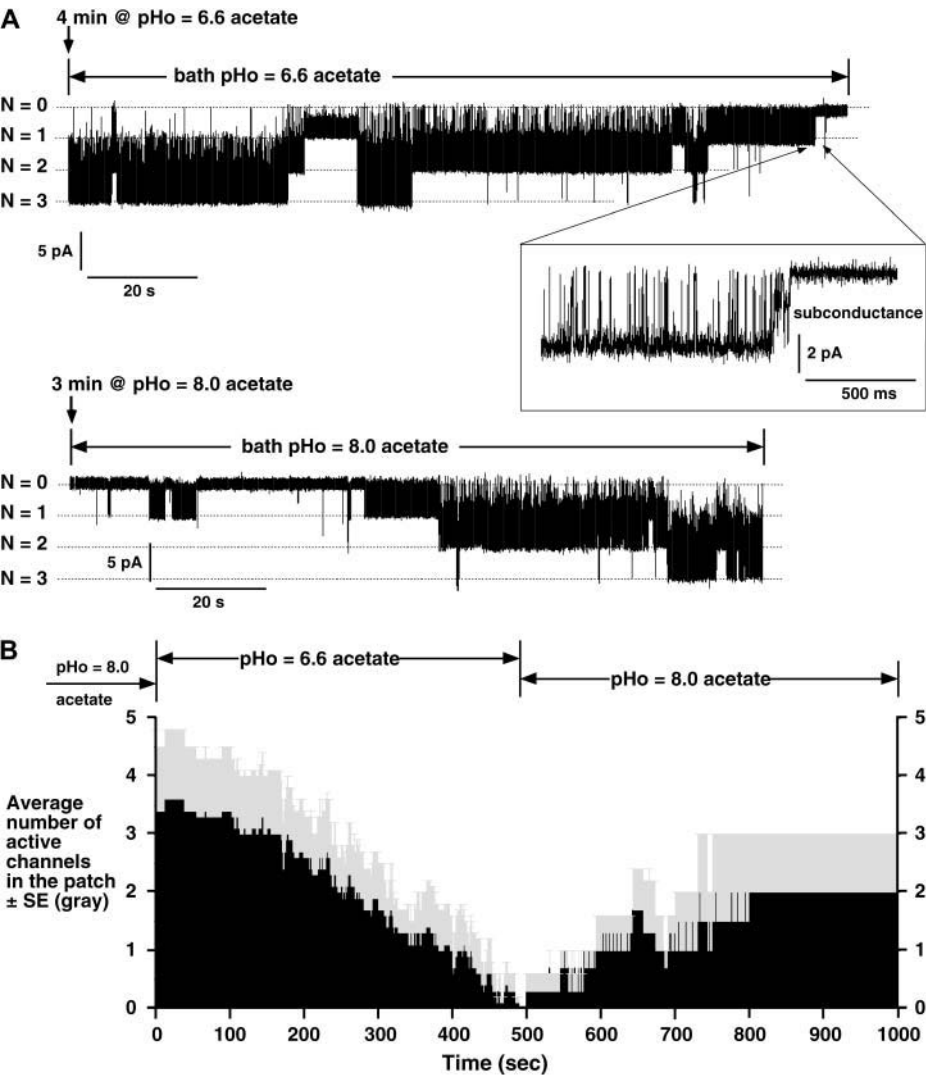
FIGURE 1 (A) Internal acidification (using external permeant buffers) reversibly closes wt-ROMK channels. Inward currents (downward deflections) were recorded at pipette holding potentials of 100 mV on cell-attached patches from *Xenopus* oocytes, depolarized by high potassium. (B) Average number of active wt-ROMK channels as a function of time, for $n = 7$ oocytes. Shaded area denotes one standard error above the mean.

pipette solution (Choe et al., 1999), and could be eliminated by using EDTA or ultrapure reagents in the pipette solutions.

The L160A mutant of ROMK is still pH-gated

Since the F146 residue in the KirBac1.1 structure might function as a steric gate (Kuo et al., 2003), we mutated the corresponding residue in ROMK (ROMK2-L160) to Ala and examined its effect on pH gating. Fig. 2 A is a representative

experiment illustrating that oocyte acidification reversibly decreased the number of active L160A channels, similar to its effect on ROMK (Fig. 1 A). Normal pH gating occurred in the L160A mutant, and there was no difference in the average timecourse of pH closure in L160A (Fig. 2 B) versus ROMK (Fig. 1 B). Moreover, the single-channel kinetics of L160A did not change during the decrease of internal pH, analogous to what was observed with ROMK (Tables 1 and 2).

TABLE 1 Single-channel kinetics of ROMK and pH-gate mutants (high pH)

	ROMK	L160A	L160G	L160G-I163M
Open probability	$0.91 \pm 0.01(5)$	0.93 ± 0.01 (6)	0.94 ± 0.01 (6)	0.87 ± 0.02 (6)
Open time (ms)	20.6 ± 0.3 (5)	20.2 ± 4 (6)	27.0 ± 4 (6)	13.6 ± 3 (4)
Closed time (ms)	1.6 ± 0.2 (5)	1.1 ± 0.1 (6)	1.3 ± 0.1 (6)	1.7 ± 0.3 (4)

All data were obtained on single-channel, cell-attached patches with 100 mM K and no divalents, in the pipette. Bath contained either 10 mM or 100 mM K. Pipette holding potential was adjusted to obtain an inward current of ~3 pA. Mean inward current for all exponents = -3.3 ± 0.1 pA. All recordings were made with acetate permeant buffers at pH 8.0. Number of oocytes is given in parentheses. Only one open state and one closed state were observed in these exponents. There were no significant differences in kinetic parameters between ROMK, L160A, and L160G ($P > 0.05$).
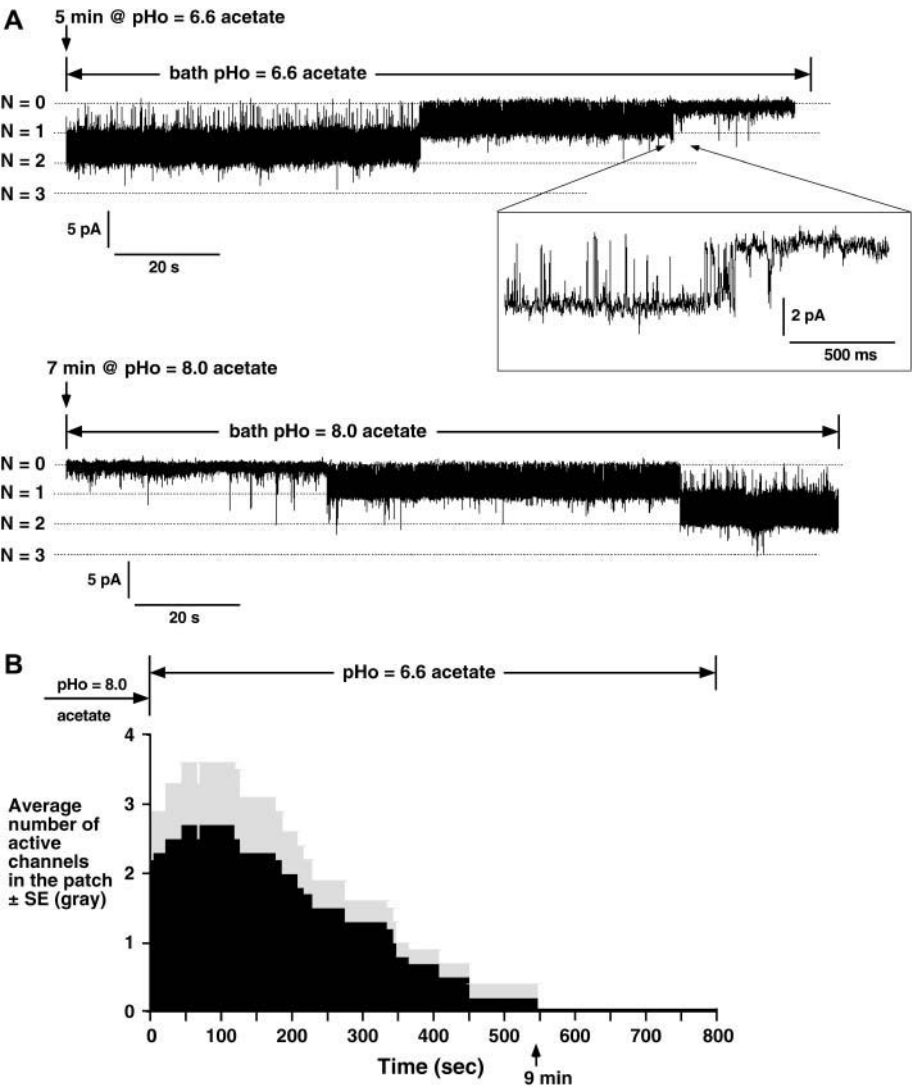
FIGURE 2 (A) Internal acidification (using external permeant buffers) reversibly closes L160A channels. Inward currents were recorded under conditions similar to Fig. 1. (B) Average number of active L160A channels as a function of time, for $n = 7$ oocytes. Shaded area denotes one standard error above the mean. In these experiments, no attempt was made to reverse channel closure by elevating pH_o.

Whole-cell recordings (using the two-electrode voltage-clamp) confirmed the single-channel pH dependence of ROMK and L160A. Whole-cell ROMK and L160A inward currents were both sigmoidal functions of pH (Fig. 3). The apparent pK_a for ROMK was $pH_o = 7.0 \pm 0.03$, corresponding to an internal pK_a of 6.6 (consistent with Fig. 7 of Sackin et al., 2003), whereas the apparent pK_a of the L160A mutant was $pH_o = 7.3 \pm 0.1$, corresponding to an internal

pK_a of 6.8. The Hill slopes for ROMK and L160A were, respectively, 3.0 ± 0.7 and 1.4 ± 0.5.

The L160G mutation disrupts pH gating in ROMK

When the normally occurring leucine at the putative pH gate (L160-Kir1.1b) was replaced by the smaller glycine the channel became generally insensitive to low internal

TABLE 2 Single-channel kinetics of ROMK and pH-gate mutants (low pH)

	ROMK	L160A	L160G	L160G-I163M
Open probability	$0.93 \pm 0.01(3)$	0.93 ± 0.01 (5)	0.94 ± 0.01 (3)	0.89 ± 0.01 (4)
Open time (ms)	18.8 ± 3 (3)	20.1 ± 2 (5)	25.2 ± 8 (3)	12.0 ± 2 (4)
Closed time (ms)	1.3 ± 0.1 (3)	0.8 ± 0.1 (5)	1.2 ± 0.2 (3)	1.2 ± 0.2 (4)

Same conditions as for Table 1, except that the pH of the permeant buffer bath was 6.6 instead of 8. ROMK and L160A kinetics were determined 1 min before channel shutdown. The kinetics of L160G and L160G-I163M were determined after 10 min at low pH. There were no significant differences in kinetic parameters among ROMK, L160A, and L160G ($P > 0.05$). Furthermore, within each clone, there were no significant kinetic differences at low pH versus high pH ($P > 0.05$) (see Table 1).
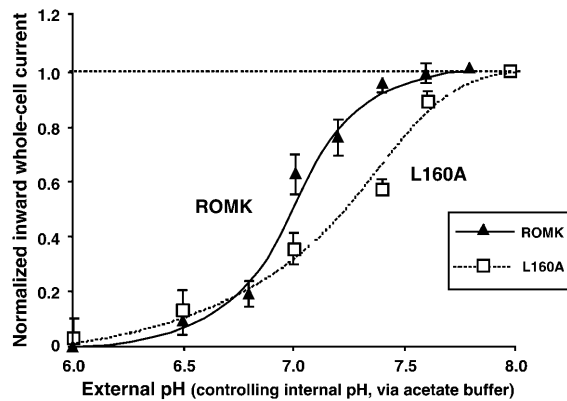
FIGURE 3 The steady-state pH gating of wild-type ROMK (Kir1.1b), and the L160A mutant at a cell potential of negative 190 mV, measured in whole oocytes using the two-electrode voltage-clamp. Large negative holding potentials were used to maximize the signal/noise ratio for the L160A currents, which averaged only 27 ± 7 μA ($n = 22$) compared with 150 ± 16 μA ($n = 12$) for wild-type Kir1.1b. Normalized inward current is plotted as a function of bath pH, which was controlled with a permeant acetate buffer. The apparent pK_a for Kir1.1b was $pH_o = 7.0 \pm 0.03$ (corresponding to an internal pK_a of 6.6) and for L160A was $pH_o = 7.3 \pm 0.1$ (corresponding to an internal pK_a of 6.8).

pH. In the example of Fig. 4, L160G-Kir1.1b channel activity persisted for an hour after bath pH_o was reduced from 8 to 6.6. In this protocol, internal pH would be expected to decrease from 7.2 to 6.3 within 9 min (see Figs. 1 and 2).

Although in most cases the L160G mutants were insensitive to pH (see Fig. 4), in a few patches some channels disappeared after prolonged exposure to an internal pH of 6.3 ($pH_o = 6.6$). In seven patches from seven oocytes, the

average number of active L160G channels decreased from 1.7 ± 0.4 to 1.3 ± 0.3 (24%) after 16 min at an internal pH of 6.3 (Fig. 5 A). In time controls at a constant $pH_o = 8$, L160G mutant channels showed no significant change in activity (1.3 ± 0.4 vs. 2.0 ± 1.0 after >16 min, Fig. 5 B). Reducing internal pH also had no significant effect on the single-channel kinetics of L160G, L160A, or ROMK until the moment of closure (Tables 1 and 2).

We also investigated the pH gating of a double mutant that combined the L160G and I163M mutations (Fig. 6). By itself, the I163M mutation shifted the apparent pK_a of ROMK more alkaline by almost 0.9 pH units (Dahlmann et al., 2004). This was confirmed in the present study, where the apparent external pK_a was 7.0 ± 0.03 for ROMK, versus 7.8 ± 0.03 for I163M. However, the double mutant I163M-L160G was essentially insensitive to internal acidification (Fig. 6).

At the single-channel level, the L160G-I163M double mutants were even less sensitive to low pH than L160G. In three patches from three separate oocytes, there were no changes in the number of active L160G-I163M channels after 30 min at $pH_o = 6.6$ in acetate-buffered bath solutions (not shown). As with the other mutants, there was no effect of internal pH on L160G-I163M kinetics (Tables 1 and 2), and no significant difference in the kinetic parameters among ROMK, L160A, and L160G.

As summarized by Fig. 6, the same 30-min acidification reduced L160G and I163M-L160G currents by respectively $22 \pm 4\%$ ($n = 16$) and $10 \pm 3\%$ ($n = 5$), compared to an almost 100% reduction of ROMK and I163M current. This highlights the importance of the L160-Kir1.1b residue in the pH-gating process.
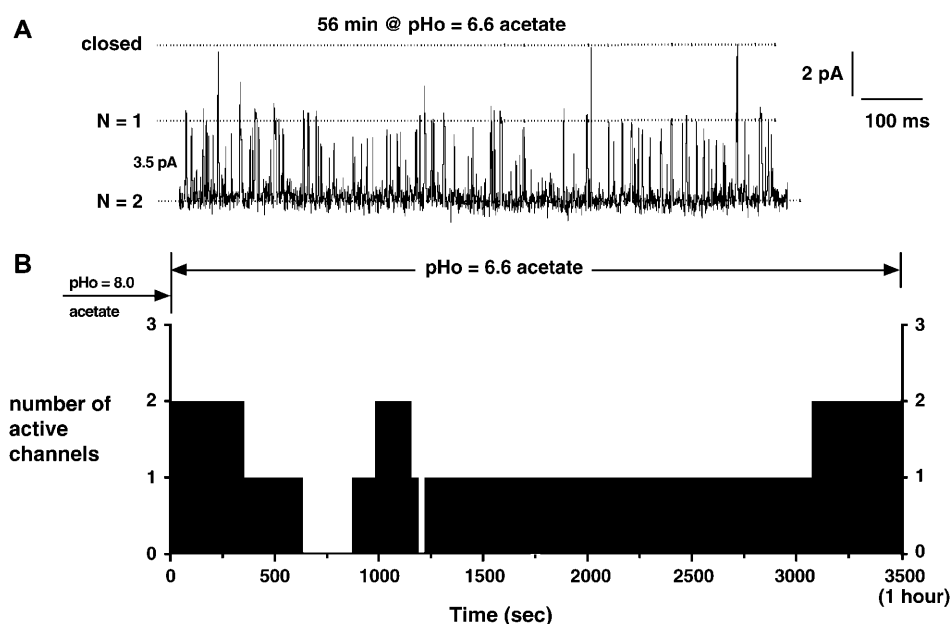

FIGURE 4 The L160G mutation on Kir1.1b alters the pH sensitivity of the channel by preventing complete closure of the pH gate. (A) Single-channel inward K current recorded at a pipette holding potential of 75 mV in a cell-attached patch. Oocyte pH was controlled with permeant acetate buffers, as described. Currents (sampled at 5 kHz and filtered at 900 Hz) are shown after 56 min at $pH_o = 6.6$, corresponding to an internal pH of 6.3. (B) Number of active channels for this patch are plotted as a function of time after changing the bath to low pH.
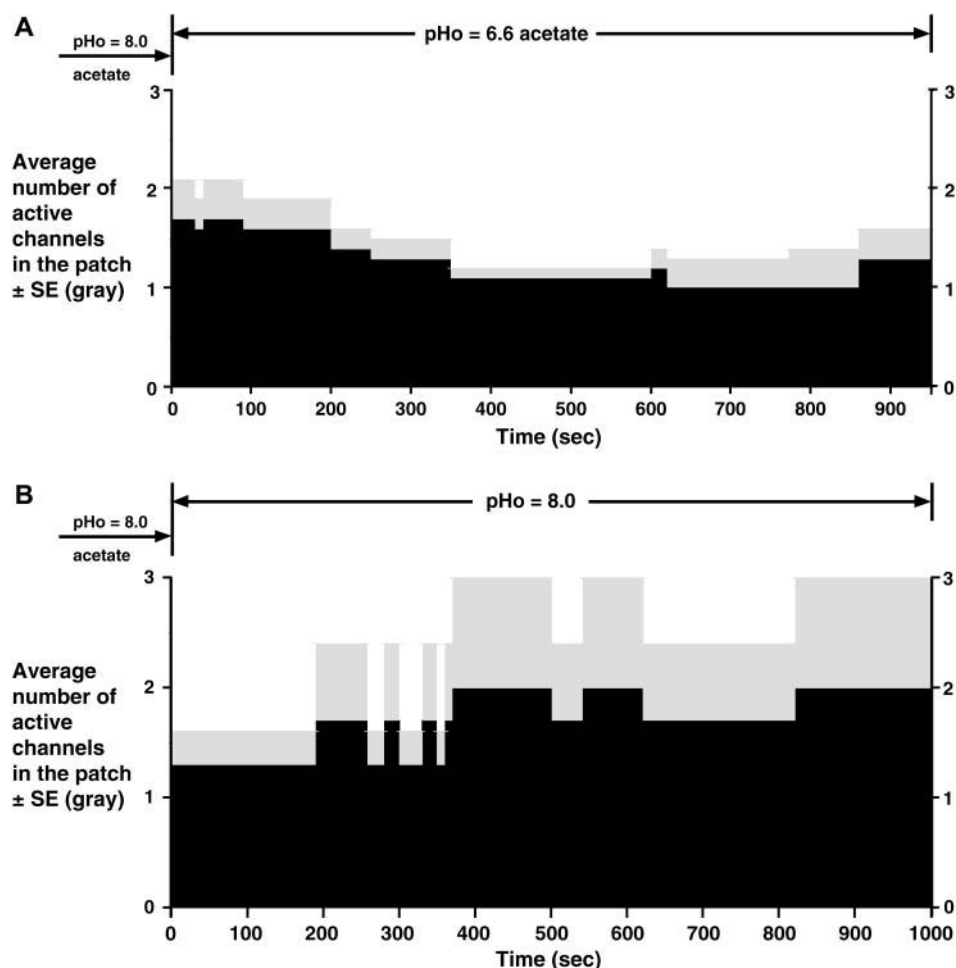
FIGURE 5 (*A*) Average timecourse for pH gating of L160G-Kir1.1b mutant channels. At time 0, bath was switched from $pH_o = 8.0$ (acetate) to $pH_o = 6.6$ (acetate). Active L160G channels declined by $24 \pm 4\%$ ($n = 7$ oocytes) over a period of 16 min. Shaded area denotes one standard error above the mean. (*B*) Time controls for L160G-Kir1.1b using the same permeant acetate buffer, except at a constant $pH_o = 8.0$.

Other side-chain substitutions at the L160 position

The Leu at the 160 position of Kir1.1b was also replaced by Met, Phe, Val, Ser, and Thr. Mutants with the hydrophobic residues Met, Phe, and Val were all more sensitive to acidification than ROMK, and their apparent pK_a increased with increasing side-chain hydrophobicity (Fig. 7). Presumably, these hydrophobic side chains prevent hydrated K ions from crossing the pH gate, thereby stabilizing the closed state of the channel. However, the wild-type Kir1.1b (ROMK in Fig. 7) does not fit this pattern since its Leu is nearly as hydrophobic as Phe. Conversely, two mutants with polar side chains (L160S and L160T) behaved similarly to L160G and L160G-I163M and did not shut down at low pH.

Single-channel conductances

Although divalents in the patch pipette did not affect the pH sensitivity of any of the channel types studied, they did affect single-channel conductance. The presence of 1 mM Mg and 2 mM Ca in the patch pipette consistently reduced the single-

channel conductance of ROMK, L160A, and L160G (Table 3). These results are similar to what has been previously reported for extracellular Mg block in Kir2.1 (Murata et al., 2002). As indicated in the table, there was no systematic significant difference in inward single-channel conductance between ROMK and the point mutants L160A, L160G, or L160G-I163M, as long as the internal and external solutions were of the same composition.

DISCUSSION

Structural locus of the ROMK2 (Kir1.1) pH gate

Results of the present study support the hypothesis that the pH gate of the mammalian Kir1.1 family (ROMK) is formed by a convergence of four Leu residues that project into the permeation path, near the bundle crossing of the inner transmembrane helices. These L160-Kir1.1b residues correspond to four F146 residues in the crystal structure of the bacterial inward rectifier KirBac1.1 (Kuo et al., 2003). Since many Kir channels have hydrophobic aromatic or aliphatic side chains at this position, it may constitute a general gate for the Kir family (Kuo et al., 2003).
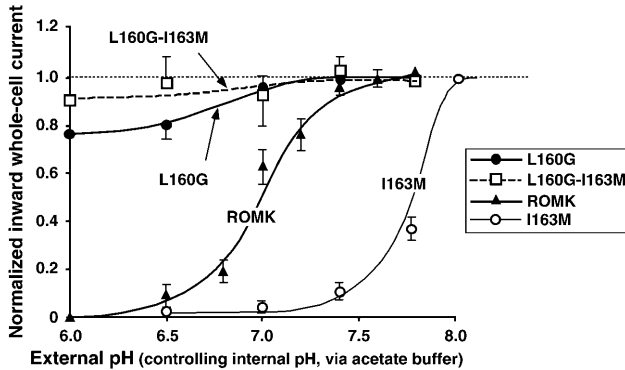
FIGURE 6 Steady-state pH gating of wild-type ROMK (Kir1.1b), and the L160 mutants, measured at a cell potential of negative 190 mV in whole oocytes, using the two-electrode voltage-clamp. Large negative holding potentials were used to maximize the signal/noise ratios for the low-expressing L160G and L160G-I163M currents, which averaged only 10 ± 2 μA ($n = 16$) and 14 ± 4 μA ($n = 7$), respectively, compared with 150 ± 16 μA ($n = 12$) for wild-type Kir1.1b. Normalized inward current is plotted as a function of bath pH, which was controlled with a permeant acetate buffer. The apparent pK_a for Kir1.1b was $pH_o = 7.0 \pm 0.03$ (corresponding to an internal pK_a of 6.6). The apparent pK_a for I163M was $pH_o = 7.83 \pm 0.03$ (corresponding to an internal pK_a of 7.1).

Fig. 8 depicts a side view of the membrane-spanning region constructed by homology-modeling Kir1.1b onto KirBac1.1 (see Methods). Two non-adjacent subunits are shown; the other two subunits would be going into and coming out of the plane of the figure. The ROMK pH sensor at K61 and the putative pH gate at L160 are indicated, together with four dehydrated K ions within the selectivity filter. As shown in the figure, the L160 residues on each subunit project into and occlude the permeation path in this closed conformation of the channel. When the permeation path is viewed from within the cytoplasm (Fig. 9 A), the ROMK homology model confirms that this path would be completely obstructed by the four L160 residues that are derived from each of the four subunits.

pH gating in Kir1.1 depends on residue 160 in ROMK2

If the four leucines at position L160 in ROMK2 constitute an essential element of the gate, mutation of these residues
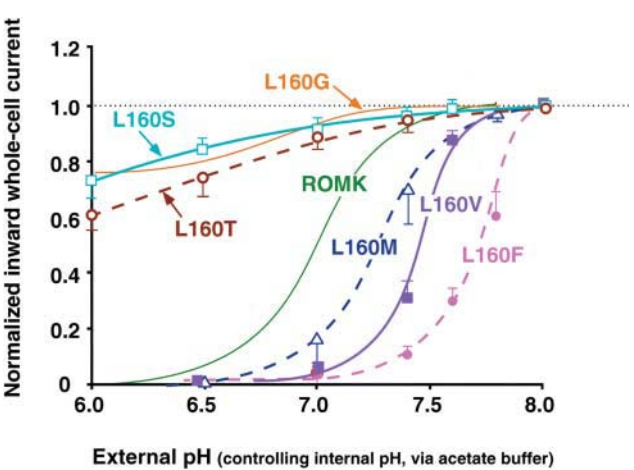

FIGURE 7 Steady-state pH gating of wild-type ROMK (Kir1.1b), and the L160 mutants, measured at a cell potential of negative 190 mV in whole oocytes, using the two-electrode voltage clamp. Normalized inward current is plotted as a function of bath pH, which was controlled with a permeant acetate buffer. The apparent pK_a for L160M was $pH_o = 7.3 \pm 0.1$ (corresponding to an internal pK_a of 6.7). The apparent pK_a for L160V was $pH_o = 7.5 \pm 0.03$ (corresponding to an internal pK_a of 6.8), and the apparent pK_a for L160F was $pH_o = 7.8 \pm 0.1$ (corresponding to an internal pK_a of 7.0). Apparent pK_a of the mutants increases with increasing side-chain hydrophobicity. The polar side chains in L160S and L160T alter pH gating similar to L160G. For comparison, the pH curves for ROMK and L160G are repeated from Fig. 6.

should affect gating. In the homology model, mutation of the Leu to the smaller Ala residue leaves enough room for a dehydrated K ion to traverse the closed gate, but not enough room for a hydrated K ion (*blue sphere*, Fig. 9 B). Since L160A pH gating (Fig. 2 B) was no different from ROMK (Fig. 1 B) at the single-channel level, K ions cannot cross a closed L160A gate by shedding their waters of hydration.

Although we do not understand why the L160A was slightly ($\Delta pK_a = 0.3$) more sensitive to acidification than ROMK, we do not believe that this reflects a major structural difference between wild-type and mutant since none of the mutants had significantly different single-channel kinetics or conductance (Tables 1–3).

In contrast to the L160A model of Fig. 9 B, the homology model for L160G indicates that there is sufficient space for

TABLE 3 Effect of external divalents on inward single-channel conductance

	ROMK	L160A	L160G	L160G-I163M
0 Mg, 0 Ca	46.7 ± 2 (7)	52.0 ± 4 (9)	38.3 ± 3 (10)	42.8 ± 5 (5)
1 mM Mg, 2 mM Ca	33.7 ± 2 (10)*	31.6 ± 1 (19)*	28.9 ± 3 (4)*	—
% block	28%	39%	25%	—

Inward single-channel conductance (pS) was measured in the linear region of the current-voltage relation between -50 and -150 mV, with external pH = 8, acetate solutions. Conductances are in pS $\pm$ SE, with the number of oocytes in parentheses. Percent block refers to the % decrease in conductance attributable to block by external divalents = $1 - (g_{divalent}/g)$.
*External divalents produced a significant reduction in conductance for each channel type ($P < 0.005$). With the same pipette solution, different channel types had no significant differences in conductance ($P > 0.05$).
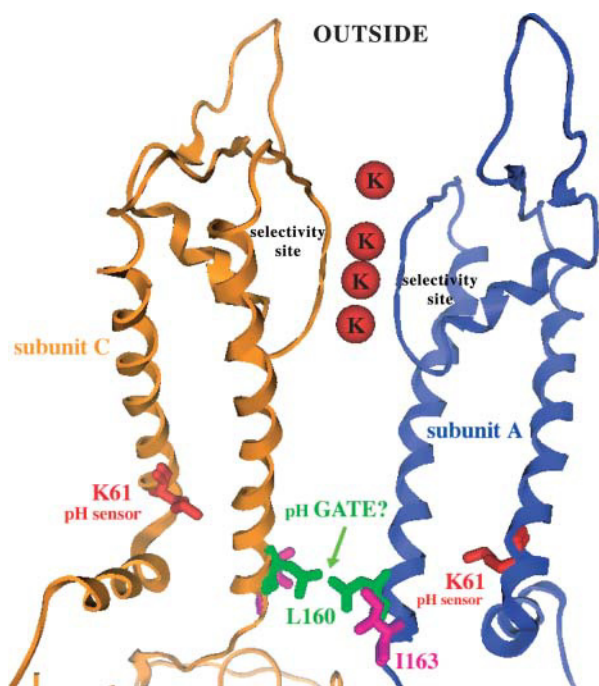
FIGURE 8 Homology model of ROMK, based on the known crystal structure of KirBac1.1. Side view, showing two of four subunits. The putative pH gate consists of four Leu 160 (Kir1.1b) residues, projecting into the permeation path at the cytoplasmic edge of the membrane, near the apical crossing of the inner transmembrane helices. Opening (and closing) of the gate could occur via rotation of adjacent subunits relative to each other or by a hinge movement of the inner helices.

both K and its hydration shell to cross the pH closed configuration of the channel (Fig. 9 *C*). This is consistent with the absence of (physiological) pH gating in the L160G mutant. Fig. 9 *C* suggests that even if low pH were to move

the Gly-160 residue into the permeation path, the glycine side chain would be too small to completely block the channel. Alternatively, it is possible that L160G eliminates hydrophobic interactions between side chains at the 160-position, thereby destabilizing the closed state of the channel relative to the open state.

To examine whether the L160G mutation alters pH sensitivity rather than gating per se, we constructed a double mutant of L160G and I163M, where the latter mutation was known to increase the apparent pKa (Dahlmann et al., 2004). The combined L160G-I163M mutant was as insensitive to pH as L160G (Fig. 6), indicating that the L160G mutation disrupts gating even when the pH sensing apparatus has been significantly altered by a second mutation (I163M). This suggests that the primary effect of L160G is on the pH gate itself.

The whole-cell pH dependence of both L160G and L160G-I163M (Fig. 6) were close to what was seen after mutation of the putative pH sensor to K61M-ROMK2 (Fakler et al., 1996; Choe et al., 1997) or with IRK1, which lacks a Lys at this position (Sabirov et al., 1997). Hence, we believe that the putative gate at L160 is somehow coupled to the pH sensor at K61, and that decreases in current at pH values below 6.0 may involve a different mechanism.

Two mutants with polar side chains (L160S and L160T) were as insensitive to acidification as L160G (Fig. 7). Presumably, polar side chains at the pH gate make the closed conformation energetically unfavorable, because their hydrophilic nature would prevent the tight packing necessary to close the permeation path. Analogous results were observed with polar substitutions at the 9′ position on the M2 helix of the nAChR channel, which is believed to form the ligand-
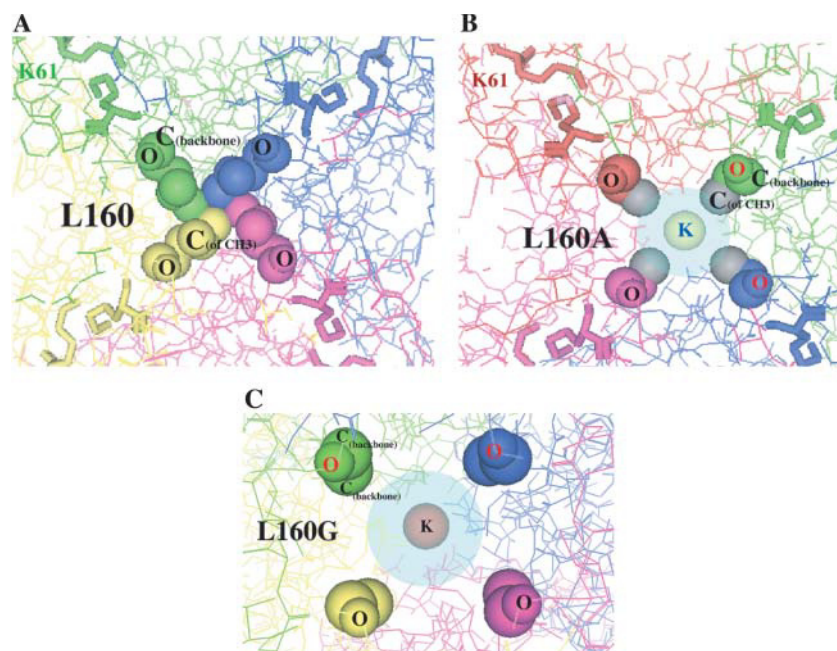

FIGURE 9 Comparison of the putative pH gate regions (*bottom view*) of (*A*) wt-ROMK, (*B*) L160A, and (*C*) L160G, as seen in the pH-closed configuration. Blue spherical shading denotes the predicted size of the hydration shell formed by eight water molecules surrounding a K ion.

dependent gate in that channel (Miyazawa et al., 2003; Labarca et al., 1995; Unwin, 1993, 2003; Kosolapov et al., 2000; Filatov and White, 1995).

Mutation of L160 does not affect single-channel conductance

As summarized in Table 3, there was no systematic difference in inward single-channel conductance in cell-attached patches from pH-open-gated ROMK, L160A, L160G, or L160G-I163M, as long as the composition of the patch pipette solution was the same. This supports the idea that mutations at the L160 position have no effect on K permeation when the pH gate is open. However, the addition of divalents to the external (pipette) solution decreased single-channel conductance in ROMK, L160A, and L160G, which is consistent with external Mg block of the open channel, as reported in previous studies on Kir2.1 (Murata et al., 2002).

Although the Ala and Gly mutations at the L160 position had no effect on single-channel conductance, they did increase rectification to the point where it was not possible to see outward K currents through L160A, L160G, or I163M-L160G. This is in marked contrast to wild-type ROMK in which outward currents were routinely detected (Sackin et al., 2004). We do not understand the reason for the apparent increased inward rectification. Specifically, we do not know if this phenomenon involves increased sensitivity to intracellular Mg^{+2} and/or internal polyamines that are responsible for the strong rectification of Kir2.1.

CONCLUSIONS

The results of single-point mutations at the L160 residue of Kir1.1b support our initial hypothesis that pH gating in the Kir1.1 family occurs when four leucines at the cytoplasmic end of the inner transmembrane helices physically occlude the permeation path. This type of gating would be similar to phenylalanine side chains blocking KirBac1.1 (Kuo et al., 2003).

We believe that the ROMK (Kir1.1) pH gate is L160-Kir1.1b because replacing these leucines with either small glycine residues or polar residues like *Ser* and *Thr* disrupted normal gating. Hence, both size and hydrophobicity of the 160-Kir1.1b residue are important for gating. Side chains that are significantly smaller or more polar than the native leucines prevent complete closure of the gate and/or stabilize the open state.

Identification of L160-Kir1.1b as the pH-gate is consistent with other results on inward rectifier channels. Spermine trapping experiments with the ATP-gated Kir 6.1 suggest that ATP closes these channels via a gate at the TM2 helix bundle crossing, near the L160 region in Kir1.1b (Phillips and Nichols, 2003). In addition, proline- and glycine-scanning mutagenesis of the GIRK4 channel implicated

F187 in TM2 as the site of closure of the G$\beta\gamma$-dependent gate (Jin et al., 2002). This residue aligns with the L160 residue of Kir1.1b. Hence, a common feature of the inward rectifier gate may be steric occlusion of the permeation path by bulky or hydrophobic side chains near the cytoplasmic apex of the inner transmembrane helices.

REFERENCES

Chanchevalap, S., Z. Yang, N. Cui, Z. Qu, G. Zhu, C. Liu, L. Giwa, L. Abdulkadir, and C. Jiang. 2000. Involvement of histidine residues in proton sensing of ROMK1 channel. *J. Biol. Chem.* 275:7811–7817.

Choe, H., L. G. Palmer, and H. Sackin. 1999. Structural determinants of gating in inward-rectifier K$^+$ channels. *Biophys. J.* 76:1988–2003.

Choe, H., H. Zhou, L. G. Palmer, and H. Sackin. 1997. A conserved cytoplasmic region of ROMK modulates pH sensitivity, conductance, and gating. *Am. J. Physiol.* 273:F516–F529.

Dahlmann, A., M. Li, Z. Gao, D. McGarrigle, H. Sackin, and L. G. Palmer. 2004. Regulation of Kir channels by intracellular pH and extracellular K: mechanisms of coupling. *J. Gen. Physiol.* 123:441–454.

Doi, T., B. Fakler, J. H. Schultz, U. Schulte, U. Brandle, S. Weidemann, H. P. Zenner, F. Lang, and J. P. Ruppersberg. 1996. Extracellular K$^+$ and intracellular pH allosterically regulate renal Kir1.1 channels. *J. Biol. Chem.* 271:17261–17266.

Fakler, B., J. H. Schultz, J. Yang, U. Schulte, U. Brandle, H. P. Zenner, L. Y. Jan, and J. P. Ruppersberg. 1996. Identification of a titratable lysine residue that determines sensitivity of kidney potassium channels (ROMK) to intracellular pH. *EMBO J.* 15:4093–4099.

Filatov, G., and M. White. 1995. The role of conserved leucines in the M2 domain of the acetylcholine receptor in channel gating. *Mol. Pharmacol.* 48:379–384.

Jin, T., L. Peng, T. Mirshahi, T. Rohacs, K. Chan, R. Sanchez, and D. E. Logothetis. 2002. The $\beta\gamma$ subunits of G proteins gate a K channel by pivoted bending of a transmembrane segment. *Mol. Cell.* 10:469–481.

Kosolapov, A., G. Filatov, and M. White. 2000. Acetylcholine receptor gating is influenced by the polarity of amino acids at position 9′ in the M2 domain. *J. Membr. Biol.* 174:191–197.

Kuo, A., J. Gulbis, J. Antcliff, T. Rahman, E. Lowe, J. Zimmer, J. Cuthbertson, F. Ashcroft, T. Ezaki, and D. Doyle. 2003. Crystal structure of the potassium channel KirBac1.1 in the closed state. *Science.* 300:1922–1926.

Labarca, C., M. Nowak, Z. Halyun, L. Tang, P. Deshpande, and H. Lester. 1995. Channel gating governed symmetrically by conserved leucine residues in the M2 domain of nicotinic receptors. *Nature.* 376:514–516.

Leipziger, J., G. MacGregor, G. Cooper, J. Xu, S. Hebert, and G. Giebisch. 2000. PKA site mutations of ROMK2 channels shift the pH dependence to more alkaline values. *Am. J. Physiol.* 279:F919–F926 (renal).

MacGregor, G. G., J. Z. Xu, C. M. McNicholas, G. Giebisch, and S. C. Hebert. 1998. Partially active channels produced by PKA site mutation of the cloned renal K$^+$ channel, ROMK2 (Kir1.2). *Am. J. Physiol.* 275:F415–F422.

Malnic, G., R. M. Klose, and G. Giebisch. 1966. Micropuncture study of distal tubular potassium and sodium transport in rat nephron. *Am. J. Physiol.* 211:529–547.

McNicholas, C., Y. Yang, G. Giebisch, and S. Hebert. 1996. Molecular site for nucleotide binding on an ATP-sensitive renal K channel (ROMK2). *Am. J. Physiol.* 271:F275–F285.

McNicholas, C. M., G. G. MacGregor, L. D. Islas, Y. Yang, S. C. Hebert, and G. Giebisch. 1998. pH-dependent modulation of the cloned renal K$^+$ channel, ROMK. *Am. J. Physiol.* 275:F972–F981.

McNicholas, C. M., W. Wang, K. Ho, S. C. Hebert, and G. Giebisch. 1994. Regulation of ROMK1 K$^+$ channel activity involves phosphorylation processes. *Proc. Natl. Acad. Sci. USA.* 91:8077–8081.

Miyazawa, A., Y. Fujiyoshi, and N. Unwin. 2003. Structure and gating mechanism of the acetylcholine receptor pore. *Nature.* 423:949–955.

Murata, Y., Y. Fujiwara, and Y. Kubo. 2002. Identification of a site involved in the block by extracellular Mg and Ba as well as permeation of K in the Kir2.1 K channel. *J. Physiol.* 544:665–677.

Palmer, L. G., H. Choe, and G. Frindt. 1997. Is the secretory K channel in the rat CCT ROMK? *Am. J. Physiol.* 273:F404–F410.

Phillips, L. R., and C. G. Nichols. 2003. Ligand-induced closure of inward rectifier Kir6.2 channel traps spermine in the pore. *J. Gen. Physiol.* 122:795–804.

Sabirov, R., Y. Okada, and S. Oiki. 1997. Two-sided action of protons on an inward rectifier K channel (IRK1). *Pflügers Arch. Eur. J. Physiol.* 433:428–434.

Sackin, H., L. G. Palmer, and M. Krambis. 2004. Potassium-dependent slow inactivation of Kir1.1 (ROMK) channels. *Biophys. J.* 86:2145–2155.

Sackin, H., S. Syn, L. G. Palmer, H. Choe, and E. Walters. 2001. Regulation of ROMK by extracellular cations. *Biophys. J.* 80:683–697.

Sackin, H., A. Vasilyev, L. G. Palmer, and M. Krambis. 2003. Permeant cations and blockers modulate pH gating of ROMK channels. *Biophys. J.* 84:910–921.

Schulte, U., H. Hahn, M. Konrad, N. Jeck, C. Derst, K. Wild, S. Weidemann, J. Ruppersberg, B. Fakler, and J. Ludwig. 1999. pH gating of ROMK (Kir1.1) channels: control by an Arg-Lys-Arg triad disrupted in antenatal Bartter syndrome. *Proc. Natl. Acad. Sci. USA.* 96:15298–15303.

Schulte, U., S. Weidemann, J. Ludwig, J. Ruppersberg, and B. Fakler. 2001. K-dependent gating of Kir1.1 channels is linked to pH gating through a conformational change in the pore. *J. Physiol.* 534:49–58.

Tsai, T. D., M. E. Shuck, D. P. Thompson, M. J. Bienkowski, and K. S. Lee. 1995. Intracellular H$^+$ inhibits a cloned rat kidney outer medulla K$^+$ channel expressed in *Xenopus* oocytes. *Am. J. Physiol.* 268:C1173–C1178.

Unwin, N. 1993. Nicotinic acetylcholine receptor at 9 Å resolution. *J. Mol. Biol.* 229:1101–1124.

Unwin, N. 2003. Structure and action of the nicotinic acetylcholine receptor explored by electron microscopy. *FEBS Lett.* 555:91–95.